INFECTION AND IMMUNITY, Sept. 2007, p. 4289–4297 Vol. 75, No. 9
0019-9567/07/$08.00+0 doi:10.1128/IAI.01679-06

Pneumococcal Cell Wall-Induced Meningitis Impairs Adult Hippocampal Neurogenesis▽

Olaf Hoffmann,[1] Cordula Mahrhofer,[1] Nina Rueter,[1] Dorette Freyer,[1] Bettina Bert,[3] Heidrun Fink,[3] and Joerg R. Weber[1,2]*

Department of Neurology[1] and Department of Cell Biology, Center for Anatomy,[2] Charité-Universitaetsmedizin Berlin, Berlin, Germany, and Institute of Pharmacology and Toxicology, Veterinary Medicine, Freie Universität, Berlin, Germany[3]

Received 20 October 2006/Returned for modification 19 December 2006/Accepted 13 June 2007

Bacterial meningitis is a major infectious cause of neuronal degeneration in the hippocampus. Neurogenesis, a continuous process in the adult hippocampus, could ameliorate such loss. Yet the high rate of sequelae from meningitis suggests that this repair mechanism is inefficient. Here we used a mouse model of nonreplicative bacterial meningitis to determine the impact of transient intracranial inflammation on adult neurogenesis. Experimental meningitis resulted in a net loss of neurons, diminished volume, and impaired neurogenesis in the dentate gyrus for weeks following recovery from the insult. Inducible nitric oxide synthase (iNOS) immunoreactivity was prominent in microglia in nonproliferating areas of the dentate gyrus and hilus region after meningitis induction. Treatment with the specific iNOS inhibitor *N*6-(1-iminoethyl)-L-lysine restored neurogenesis in experimental meningitis. These data suggest that local central nervous system inflammation in and of itself suppresses adult neurogenesis by affecting both proliferation and neuronal differentiation. Repair of cognitive dysfunction following meningitis could be improved by intervention to interrupt these actively suppressive effects.

Neurogenesis, the production of new neurons from precursor cells, remains constitutively active throughout adult life in defined regions of the mammalian brain, e.g., the subgranular zone (SGZ) of the dentate gyrus (DG) and the subventricular zone (SVZ). Neurogenesis can be induced by physiological stimuli, e.g., physical exercise (24, 50), but is also modulated in pathological conditions such as focal or global cerebral ischemia (23, 28), traumatic brain injury (10), and epileptic seizures (35). Neurogenesis has been studied as a potential repair mechanism for brain damage of diverse origins. For example, treatment with fibroblast growth factor 2, epidermal growth factor, or transforming growth factor α (14, 32, 56, 57) has been attempted to increase neurogenesis after injury. Anti-inflammatory treatment with indomethacin (30) or minocycline (12) promotes neurogenesis in the face of systemic inflammation induced by lipopolysaccharide (LPS).

Bacterial meningitis is the prototype of acute intracranial inflammation associated with neuronal damage in the DG (6). Even with modern antibiotic treatment, it is still a life-threatening disease leading to frequent sequelae. Fifty percent of the survivors suffer from neuropsychological deficits (3), which have been linked to the loss of neurons predominantly in hippocampal structures in patients and experimental models (33). Replacement of lost neurons in the natural course of recovery from meningitis has not been well studied.

Streptococcus pneumoniae is the most common pathogen causing meningitis associated with an unfavorable clinical outcome. In pneumococcal meningitis, bacterial toxins such as the pore-forming pneumolysin and hydrogen peroxide induce half of the neuronal damage (6). Equally important, however, is antibiotic-induced lysis of bacteria that leads to a massive release of bacterial cell wall components (16). Recognition of the bacterial cell wall, which is composed of teichoicated peptidoglycan and lipoteichoic acid (47), by Toll-like receptor 2 is currently regarded as the predominant pathway by which pneumococci stimulate the immune response (43, 53, 55). The concentration of major cell wall components in the cerebrospinal fluid (CSF) correlates with disease severity in pneumococcal meningitis (42), and the clinical situation may worsen even in the absence of viable bacteria (41, 45, 48). Our model features the major host-side hallmarks of meningitis (29, 53). Induction of meningitis by injection of chemically defined cell wall (21) allows study of the effects of local and temporally limited central nervous system (CNS) inflammation. In contrast, meningitis induced by live bacteria is characterized by a pronounced systemic inflammatory response, suggesting that circulating factors such as interleukin 6 (30) may act as additional modulators of neurogenesis. The aim of this study was to demonstrate the impact of acute intracranial inflammation on constitutive neurogenesis in the DG, to identify potential host-side mechanisms, and to determine the net restorative effect on experimental meningitis-induced neuronal loss in the DG. A limitation is that this approach may not be fully representative of meningitis induced by live pathogens, in which additional effects of the bacterial metabolism could be hypothesized.

MATERIALS AND METHODS

Preparation of PCW. Pneumococcal cell wall (PCW) was prepared as previously published (48, 53). Briefly, unencapsulated pneumococci (strain R6) were cultivated overnight in casein-plus-yeast medium at 37°C with 5% CO_2. Following heat inactivation, bacteria were mechanically disintegrated. The suspension was digested with 10 μg/ml DNase (Promega, Mannheim, Germany) and 50 μg/ml RNase (USB Corp., Cleveland, OH) for 1 h at 37°C, followed by treatment with 0.01% trypsin (Sigma) for 2 h at 37°C. The digest was sedimented by centrifugation (23,000 × *g*, 20 min) and resuspended in 2% sodium dodecyl

* Corresponding author. Mailing address: Department of Cell Biology, Center for Anatomy, Charité-Universitaetsmedizin Berlin, Schumannstr. 20/21, 10117 Berlin, Germany. Phone: 49 30 450 528002. Fax: 49 30 450 528902. E-mail: joerg.weber@charite.de.

▽ Published ahead of print on 25 June 2007.

TABLE 1. Experimental group design for histological studies

Group	No. of mice		BrdU treatment days[a]	Sacrifice day[a]	Treatment
	Control	Meningitis			
1	7	9	0–2	3	None
2	6	7	0–2	3	L-NIL
3	7	9	21–23	24	None
4	6	7	21–23	49	None
5	9	7	35–37	38	None

[a] Day 0 was the day of challenge with cell wall.

sulfate (Serva, Heidelberg, Germany) at 90°C for 20 min, followed by eight cycles of washing. LPS was not detectable using a commercially available *Limulus* amebocyte lysate assay (Whittaker Bioproducts, Walkersville, MD). The optical density (absorption at 620 nm) of the solution was adjusted to 1.0, which was equivalent to 10^8 CFU per ml (49, 53). The chemical composition of this cell wall has been published previously (17).

Animal experiments. All animal experimental protocols were reviewed and approved by state authorities. Meningitis was induced in 8-week-old male 129S6 mice weighing approximately 20 g by instillation into the lumbar spinal canal of 40 μl PCW preparation, using a previously published protocol (21). (These mice are referred to as meningitis mice below.) Controls received an equal volume of pyrogen-free phosphate-buffered saline (PBS). Adequate waking from anesthesia and absence of pareses were verified. To exclude effects of anesthesia or of the surgical procedure, untreated mice were studied as further controls. To label proliferating cells, five doses of bromodeoxyuridine (BrdU) (50 mg/kg) were given intraperitoneally (i.p.) at 12-h intervals over three consecutive days prior to sacrifice. Doses of 50 mg/kg BrdU were previously demonstrated to yield near-saturation labeling and are considered to give reliable results also in pathological conditions (7). Repeated injections rather than single-point labeling were used to allow study of the cumulative effects of the acute inflammatory period (30).

A subset of animals was treated with the specific inducible nitric oxide synthase (iNOS) inhibitor *N*6-(1-iminoethyl)-L-lysine (L-NIL) (Alexis Biochemicals, Grünberg, Germany), which was added to the drinking water at 1 mg/ml until sacrifice (39, 51) and given i.p. (0.1 mg/kg in sterile PBS) as a loading dose at the time of surgery. In the behavioral studies, mice received L-NIL until after testing. L-NIL has no reported activity on endothelial NOS and has a 28-fold specificity over the neuronal isoform (31). At the end of the experiment, animals were deeply anesthetized and sacrificed by transcardial perfusion with PBS. Brains were removed and snap frozen in methylbutane on dry ice. The group design, times of BrdU labeling, and survival intervals are shown in Table 1.

Measurements of cytokines and corticosteroids in serum. To determine the degree of systemic inflammation elicited by the intrathecal injection technique, we measured the concentrations of interleukin 1β and interleukin 6 in the sera of control mice as well as 3 h and 24 h after intrathecal challenge with PCW. Measurements were performed using mouse-specific commercial enzyme-linked immunosorbent assay kits (Ebioscience, San Diego, CA). Furthermore, we studied the effect of experimental meningitis on the serum concentrations of corticosterone and cortisol in order to rule out confounding effects of these the stress hormones on neurogenesis. Cortisol was measured in pooled sera from PBS-injected controls ($n = 10$) or meningitis mice ($n = 10$) at 12 h after surgery, using a commercially available assay (Immulite 2000; Diagnostic Products Corporation, Los Angeles, CA). Corticosterone was measured in individual samples from PBS controls ($n = 10$) or meningitis mice ($n = 10$) after 12 h, using a commercial enzyme-linked immunosorbent assay (Cayman Chem, Ann Arbor, MI).

Sectioning and immunohistology. All staining was performed on 20-μm thaw-mounted cryosections spanning the entire hippocampus of both hemispheres. For quantification of immunolabeled cells, every 10th section was studied. Stereological estimates were obtained from the left DG only, using every 20th section. Proliferation in the DG was determined by light microscopic quantification of BrdU immunostaining. For this purpose, slides were air dried and postfixed for 10 min in 4% freshly made paraformaldehyde in PBS. After blocking with 3% normal goat serum and 0.3% Triton X-100 in PBS, slides were incubated with 2 N HCl for DNA denaturation. Slides were rinsed in PBS and incubated with a rat monoclonal antibody against BrdU (Chemicon, Chandlers Ford, United Kingdom; 1:250 in blocking solution) at 4°C overnight. For visualization, a biotinylated goat anti-rat immunoglobulin G (IgG) and ABC peroxidase kit (Vector Laboratories; Linaris, Wertheim-Bettingen, Germany) were used following the manufacturer's instructions. Diaminobenzidine (Sigma) was used as the chromogenic substrate. Slides were then counterstained with hematoxylin.

To study neuronal differentiation of newly formed cells, slides pretreated as described above were incubated with primary antiserum against NeuN (mouse monoclonal; Chemicon; 1:100 in blocking solution), a marker of mature neurons, or Hu-D (rabbit polyclonal; Chemicon; 1:100 in blocking solution), which is expressed early in immature neurons. Astrocytes were identified by glial fibrillary acidic protein (GFAP) (rabbit polyclonal; Dako, Hamburg, Germany; 1:500 in blocking solution). In the case of NeuN, background was reduced by preincubation with an anti-mouse IgG blocking reagent (Mouse On Mouse kit; Vector Laboratories). Signal was visualized using appropriate Alexa-488-labeled secondary antibodies (Invitrogen, Karlsruhe, Germany) followed by BrdU immunostaining. BrdU signal was visualized using a Texas red-labeled goat anti-rat secondary antibody.

Other antibodies used in this study were rabbit anti-iNOS (BD Transduction Labs, Heidelberg, Germany; 1:1,000), rabbit anti-active caspase 3 (BD Pharmingen, Heidelberg, Germany; 1:250), rabbit antinitrotyrosine (Upstate; Biomol, Hamburg, Germany; 1:100), rat monoclonal anti-CD11b (Chemicon; 1:100), and mouse monoclonal antinestin (Chemicon; 1:250). For visualization of rabbit IgG, a Texas red secondary antibody (Vector Laboratories; 1:100) was used. In some slides, mouse or rat IgG was visualized using appropriate biotinylated goat antisera (Vector Laboratories) followed by a streptavidin-aminomethyl coumarin conjugate (Vector Laboratories, 1:100). In further sections, Hoechst 33258 (1:10,000; Molecular Probes) was used as a nuclear counterstain. The distance between newly formed cells in the DG and sites of peroxynitrite formation was determined by fluorescence microscopy at a magnification of ×1,000 on slides double stained for BrdU and 3-nitrotyrosine, using a measuring tool included in the Stereo Investigator software (MicroBrightfield Germany, Magdeburg).

Cell counting and determination of DG volume. Cell counting was performed in two ways. The absolute number of BrdU-positive nuclei in both DGs was determined by light microscopy at a magnification of ×1,000, including cells in the granular and subgranular layers and in the white matter up to one cell width away from the inner border of the granular zone. Counting was performed on 20-μm sections spaced 200 μm apart, including the entire DG. Active caspase-3-positive cells in the DG were counted by fluorescence microscopy using the same protocol. To determine the relative proportion of BrdU-positive cells in the DG with neuronal (NeuN or Hu-D) or astrocytic (GFAP) differentiation markers, 100 BrdU-positive cells per animal were examined for double fluorescence at a magnification of ×1,000. Estimates of the DG volume and number of DG neurons were obtained using Stereo Investigator software on a Leica DM-RA microscope equipped with a motorized stage controller. DG volume was determined according to the Cavalieri principle as implemented in the Stereo Investigator software. For this purpose, the area of the DG was manually delineated on each section using a ×20 objective. For cell counting, a ×100 objective with a numerical aperture of 1.4 was used. We applied the optical fractionator with a counting box of 20 by 20 μm and a sampling grid of 100 by 170 μm, studying hematoxylin-stained sections at 400-μm intervals. Since shrinkage of fresh-frozen tissue leads to nonhomogenous, unpredictable reduction of the section thickness, the fractionator was modified as suggested by Williams and Rakic (http://www.nervenet.org/papers/3DCounting.html) in that both the section thickness and height of the counting box were set to 20 μm, omitting top and bottom guard zones ("quick-fix method"). This strategy may lead to a systematic overestimation of the neuronal density and absolute number of neurons per animal but allows reliable group comparisons.

To determine the number of BrdU-positive nuclei in the SVZ, 20-μm consecutive sections were prepared as described above, including the levels between the genu corporis callosi and the crossing of the comissura anterior. Using every 10th section, the optical fractionator was applied accordingly with a counting box of 20 by 20 μm and a 100- by 150-μm grid.

Behavioral studies. In the Morris water maze task (1), the mice underwent a single adaptation trial on day 0. They were released into the pool for 90 s, with no escape platform present. On the following 8 days (days 1 to 8, "place version"), a transparent platform (10 by 10 cm) was placed 1 cm below the surface in the middle of one of four virtual quadrants. Each day the animals were lowered into the water facing the wall from three different starting points. Animals which did not find the escape platform within 90 s were placed on it and remained there for 30 s for orientation. Afterwards they were removed to rest for 60 s. For each trial, the search time (escape latency) and path length to reach the platform were measured by a computerized tracking system (TSE VideoMot, version 1.43, Germany), and the average swimming speed was calculated. For each mouse the three daily trials were averaged. On day 9 the escape platform was removed ("spatial probe"), and the time spent in each quadrant during a single 90-s trial was registered. On the 10th day ("cued version") the platform

was elevated 1 cm above water level, signaled by a white cylinder (3 cm in diameter and 4 cm high), and moved to the quadrant opposite to the initial quadrant. Following completion of the water maze studies, a pause of 7 days was introduced in order to avoid possible carryover effects to the subsequent hole board study. The automated hole board apparatus (Tru Scan 99; Coulbourn Instruments) consists of a square box (28 by 28 cm) made of translucent Perspex with 16 equally spaced holes (2.2 cm in diameter and 2 cm deep) in a rough-textured aluminum floor. Two photobeam sensor rings were used to record the number of nose pokes and the distance traveled. The hole board was illuminated by a neon lamp (400 lx) embedded into the ceiling. The test was conducted on two consecutive days, and animals were placed in the center of the apparatus and observed for 10 min. After use by each animal, the box was cleaned with 30% (vol/vol) 2-propanol. Habituation to the apparatus was defined as a significant reduction of nose pokes and locomotor activity from the first to the second day (52).

Additional groups of control mice ($n = 14$), meningitis mice ($n = 12$), and L-NIL-treated meningitis mice ($n = 13$) were individually tested in an inhibitory avoidance paradigm, starting 3 weeks after meningitis induction. For a single training session, mice were placed in a step-through apparatus consisting of a larger illuminated start compartment and a smaller dark compartment (shock compartment). During the training, the mouse received an unavoidable foot shock (1 s, 0.1 mA) after crossing over into the dark compartment. Mice with initial step-through latencies of longer than 60 s were rejected from further experimentation. Twenty-four hours later, the mice were again released into the illuminated start compartment, and the step-through latency was recorded. The experiment was terminated after 180 s if a mouse did not cross into the dark compartment (successful learning).

Statistical evaluation. Statistics were performed using SigmaStat statistical software (SPSS Inc., Chicago, IL). All data are presented as means ± standard deviations. Multigroup comparisons were performed by one-way analysis of variance (ANOVA) followed by Student-Newman-Keuls post hoc testing. In the water maze experiments, data were analyzed by two-way ANOVA followed by the Holm-Sidaks method for post hoc multiple pairwise comparisons for place version and cued version. Spatial probe data were analyzed by repeated-measures two-way ANOVA, and Holm-Sidaks post hoc testing was used. After ensuring normal distribution and equal variance, a paired t test was used for the hole board data. Fisher's exact test was used to compare percentages in the inhibitory avoidance test. A P value of <0.05 was considered a significant difference.

RESULTS

Effect of meningitis on proliferation and neurogenesis. Our first aim was to identify time-dependent changes of the rate of precursor cell proliferation and constitutive neurogenesis in the SGZ of the DG after induction of meningitis. Proliferating cells in the SGZ were identified by the incorporation of BrdU over 3 days. During the study period, we observed a decline in baseline proliferation in control mice after intrathecal injection of PBS (3 days after surgery, 14,859 ± 3,288 BrdU-positive cells; 3 weeks, 7,640 ± 2,271 cells; and 5 weeks, 6,512 ± 892 cells in both SGZs [$P < 0.01$]). A similar age-dependent decline was found also in mice which were untreated except for BrdU injections (8 weeks old, 14,389 ± 2,742 BrdU-positive cells; 13 weeks old, 6,433 ± 3,032 cells [$P < 0.01$]). These findings reflect the relatively young age of the mice (8 weeks) at the beginning of the experiment. Compared to time-matched PBS-injected controls, meningitis led to a significant reduction of BrdU-immunopositive nuclei in the SGZ on day 3 after intrathecal challenge, followed by an increase of proliferation at 3 weeks and a return to equivalent numbers of BrdU-positive cells compared to controls at 5 weeks (Fig. 1A; see Fig. 3A). In the SVZ, a similar reduction of BrdU-positive cells was observed 3 days after meningitis induction (controls, 142,438 ± 29,784; meningitis, 108,250 ± 33,901 [$P = 0.027$]) (see Fig. 3B). Later time points were not studied in the SVZ.

Newly formed cells adopting a neuronal fate were identified by double labeling for BrdU and the early expressed neuronal differentiation marker Hu-D (Fig. 1B; see Fig. 3C). The proportion of newly formed cells expressing the neuronal differentiation marker was significantly lower in the meningitis group both at 3 days (48% ± 4% versus 54% ± 5%; $P < 0.01$) and at 3 weeks (44% ± 2% versus 55% ± 2%; $P < 0.01$) (Fig. 1B) after meningitis induction. By comparison, the proportion of BrdU-positive cells colabeled with the astrocytic marker GFAP was 5% ± 1% versus 6% ± 1% at 3 days (not significant) and 14% ± 2% versus 19% ± 2% at 3 weeks ($P < 0.01$). These data indicate that meningitis led to a decrease in proliferation and neurogenesis in the SGZ on day 3. This was followed by a transient increase of proliferation at 3 weeks after meningitis induction but a continued reduction of neuronal differentiation together with a significant increase of gliogenesis.

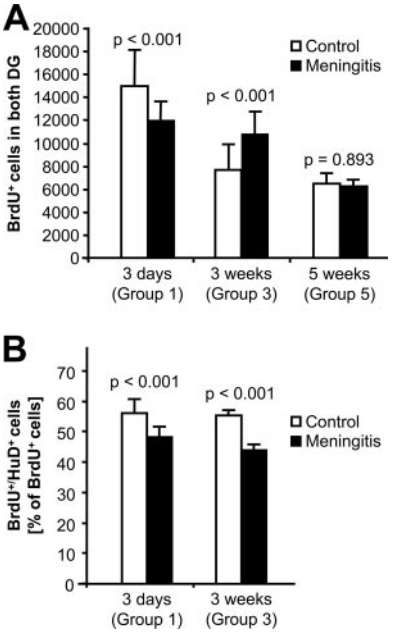

FIG. 1. Rate of proliferation of new neurons following acute meningeal inflammation. (A) Nuclei in both DG that accumulated BrdU over 3 days were enumerated. (B) The percentage of BrdU-positive cells expressing the early neuronal differentiation marker Hu-D was determined at 3 days and 3 weeks after meningeal challenge with cell wall. P values were calculated by one-way ANOVA followed by Student-Newman-Keuls post hoc testing.

Long-term effects of meningitis on neuronal cell count and DG volume. Next, we asked whether the transient increase of proliferation at 3 weeks could compensate for the acute meningitis-associated neuronal loss. We performed stereological estimates of the absolute neuronal cell count in the DG (Fig. 2A) and of the DG volume (Fig. 2B). Three days after CSF challenge, no statistically significant difference in the total neuronal cell count was detected between the meningitis and control groups (Fig. 2A). In the control animals (given PBS intrathecally), an increase of the total neuronal cell count was demonstrated at 3 and 5 weeks after challenge compared to baseline at 3 days ($P < 0.001$ for both time points). This finding is consistent with the young age of the mice at the beginning of the experiment. The neuronal cell count was significantly lower

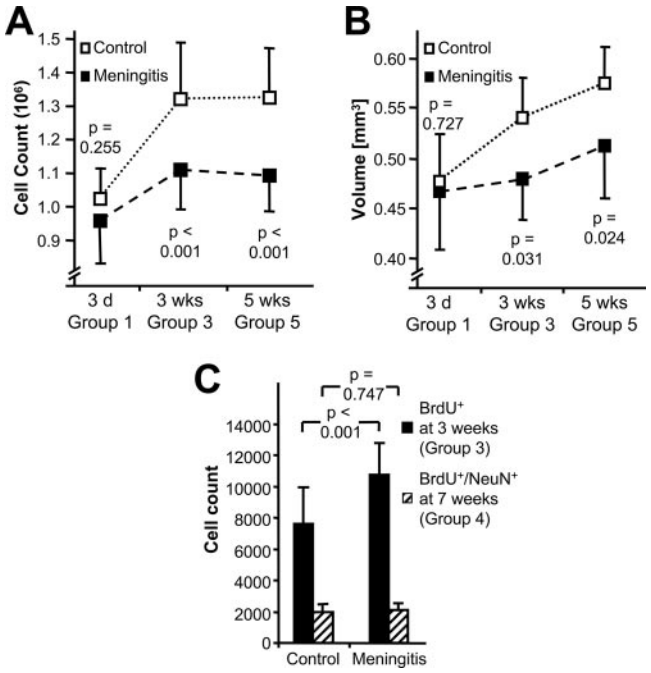

FIG. 2. Effects of meningitis on hippocampal growth. (A and B) The absolute number of granule cells (A) and volume (B) of the DG bilaterally were compared over a 5-week observation period in mice with and without challenge with PCW. (C) To follow the long-term fate of new neurons appearing after cell wall challenge, all animals received BrdU on days 21 to 23 after surgery. Although meningitis animals (solid bars) showed an increase of BrdU-positive cells in the DG on day 24 compared to control animals (hatched bars), equal numbers of newly formed neurons were present in both groups 4 weeks later. *P* values were calculated by one-way ANOVA followed by Student-Newman-Keuls post hoc testing.

in the meningitis group at 3 weeks ($P < 0.001$) and 5 weeks ($P = 0.002$) after inoculation compared to time-matched controls. Additionally, only a minor increase in neuronal cell count was observed during the study period (at 5 weeks, $P = 0.069$ compared to day 3).

Next we determined the effect of meningitis on the DG volume (Fig. 2B). Control animals showed a significant increase of DG volume (by about 20%) at 5 weeks after surgery ($P < 0.001$), a finding not observed in meningitis animals ($P = 0.233$). Meningitis was followed by a significantly smaller DG volume compared to control animals after 3 weeks ($P = 0.031$) and 5 weeks ($P = 0.024$).

In addition, we studied the survival of those early neurons formed 3 weeks after meningitis induction. Mice received BrdU labeling on days 21 to 23 and were left to survive for 4 weeks. We used double immunolabeling for BrdU and the mature neuronal marker NeuN to identify neurons which had been generated at 3 weeks after surgery and were still present at 7 weeks (Fig. 2C and Fig. 3D). In these animals, the number of BrdU and NeuN double-positive cells did not differ between meningitis mice and PBS-injected controls (1,993 ± 490 in controls and 2,080 ± 458 in meningitis mice; $P = 0.75$) (Fig. 2C). Thus, compared to the cell counts in animals studied immediately after labeling at 3 weeks postchallenge, more newly formed cells had disappeared in the meningitis group at 7 weeks than in PBS-injected controls. Together, these findings suggest that the increase in proliferation at 3 weeks after meningeal challenge does not translate into a net gain of newly formed neurons or lead to a replacement of neuronal loss after meningitis.

Role of precursor cells. We then investigated potential mechanisms which might contribute to the decrease of BrdU-positive cells at 3 days after meningitis induction. First, we looked for histological evidence of damage to precursor cells by using double labeling for nestin, a marker of neuronal/astrocyte precursor cells, and activated caspase 3, a marker of apoptosis (Fig. 3E). Compared to PBS-injected controls, we observed an increase of active caspase 3-immunopositive cells in the meningitis group, localized mainly to the inner layers of the DG and the hilar region (Fig. 3E and F). Precursor cells could be identified by nestin immunopositivity and typical astrocyte-like processes, but nestin did not colocalize with active caspase 3 signals (Fig. 3E). Interpretation of the nestin signal was impaired by additional (specific) staining of blood vessels by the nestin antibody (15) and the distribution of the nestin signal mainly to the cellular processes, precluding a reliable comparison of the number of nestin-positive cells between groups (15).

Alternatively, we hypothesized that a special vulnerability of newly formed cells to the inflammatory environment could lead to reduced numbers of BrdU-positive cells at 3 days after meningitis induction. We performed costaining for BrdU and active caspase 3 and included NeuN as a third marker to identify the type of active caspase 3-positive cells (Fig. 3F). Meningitis was associated with an increase of apoptosis. At 3 days after surgery, 218 ± 56 cells in both DGs were immunopositive for active caspase 3 in controls, compared to 553 ± 102 cells in meningitis mice ($P < 0.001$). The vast majority of apoptotic cells were identified as mature neurons by immunopositivity for NeuN. Conversely, no BrdU-positive cells were labeled by the active caspase 3 antibody. These results indicate that apoptosis of precursor cells or of newly formed cells is not the principal mechanism of reduced proliferation and neurogenesis at 3 days after meningitis induction.

Activation of microglia and nitric oxide. We hypothesized that the acute reduction of proliferation and neurogenesis in the SGZ at 3 days after meningitis induction could be related to an inflammatory environment and that nitric oxide (NO) produced by immunocompetent cells could be involved as a mediator. We performed double staining for BrdU and CD11b, a surface marker that is upregulated on activated microglia. The number of CD11b-positive cells in the hippocampus was strongly increased 3 days after meningitis induction (Fig. 3G) compared to that in controls (Fig. 3H). In meningitis animals, BrdU-positive cells were rarely found in proximity to CD11b-positive cells. The average distance from CD11b-positive cells to the nearest BrdU-positive cell within individual sections was 48.5 ± 23.4 μm, with the minimal distance being 21 μm. To study whether microglia may be a relevant source of NO in meningitis, we performed double staining for CD11b and iNOS, the key enzyme of inflammatory NO production. iNOS protein was expressed mainly in CD11b-positive cells in the DG 3 days after meningitis induction (Fig. 3I), whereas no expression of iNOS protein was found in controls (Fig. 3J). To demonstrate activity of the enzyme, we performed immunostaining for nitrotyrosine, a footprint of NO-

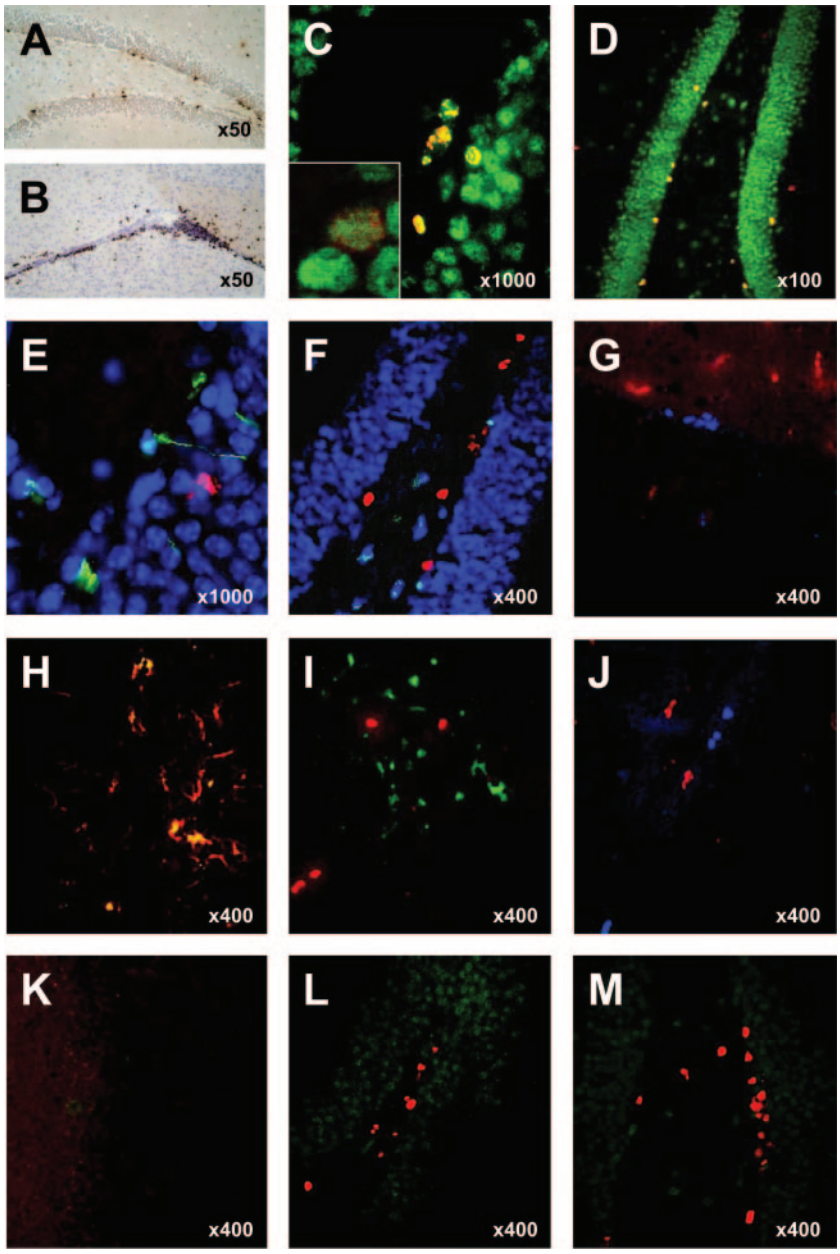

FIG. 3. Immunohistology of the DG. (A and B) Bright-field microscopic BrdU immunostaining was used to quantify newly formed cells in the DG (A) and SVZ (B). (C) Double staining for BrdU (red) and Hu-D (green) immediately after BrdU exposure was used for the early quantification of newly formed cells adopting a neuronal phenotype. Inset, confocal demonstration of colocalization. (D) Double staining for BrdU (red) and NeuN (green) 4 weeks after BrdU exposure was used to quantify surviving new neurons. (E) Apoptosis of NPCs was examined 3 days after meningitis induction by costaining for activated caspase 3 (red), nestin (green), and chromatin (blue). (F) Triple staining for active caspase 3 (green), NeuN (blue), and BrdU (red) 3 days after meningitis was used to indicate apoptosis of mature neurons. (G and H) Double staining for BrdU (blue) and CD11b (red) revealed more CD11b-positive microglia 3 days after meningitis (G) compared to the control (H) but no colocalization of proliferating cells with these activated microglia. (I and J) Activated microglia (CD11b, green) expresses iNOS protein (red) in meningitis mice (I) but not in controls (J). (K through M) Double staining for BrdU (red) and nitrotyrosine (green), a footprint of peroxynitrite, reveals nitrotyrosine formation in untreated meningitis (K) but not in controls (L) or in meningitis mice treated with the iNOS inhibitor L-NIL (M).

derived peroxynitrite. The nitrotyrosine signal was strongly increased in the DG at 3 days after meningitis induction (Fig. 3K) compared to that in controls (Fig. 3L). In sections double stained with anti-BrdU, proliferating cells were usually not found close to sites of NO production (Fig. 3G). The average distance within individual sections was 50.1 ± 30.3 μm. Our findings show that the reduction of BrdU-positive cells at 3 days after meningitis induction is paralleled by the presence of activated, iNOS-positive microglia and increased local NO production.

Role of cytokines and stress hormones. By selecting a sterile bacterial cell wall preparation as a challenge, we aimed at inducing a self-limited, strictly intrathecal inflammation. To

verify the absence of a significant systemic inflammatory response, we measured the serum concentrations of proinflammatory cytokines. Interleukin 1β was below the detection limit of 8 pg/ml in control mice as well as 3 h and 24 h after induction of experimental meningitis. Interleukin 6 was below the detection limit of 4 pg/ml in controls. A very slight increase to 130 ± 136 pg/ml was observed 3 h after challenge, which subsided within 24 h in most animals (to 28 ± 40 pg/ml). By comparison, systemic challenge with LPS induces peak levels of interleukin 6 in the nanogram to microgram range within 3 h (27). To address the issue of whether effects of meningitis on proliferation and neurogenesis might be secondary to changes of stress hormones, we compared the serum concentrations of corticosterone and cortisol in control and meningitis mice. At 12 h after challenge, we did not detect a relevant difference for corticosterone (36.8 ± 8.8 versus 38.8 ± 8.3 ng/ml; $P = 0.6$) or cortisol (49 versus 47 pmol/liter; measured in pooled sera).

Restoration of neurogenesis by iNOS inhibition. To further support a causal role of inflammatory NO, we tested whether treatment with L-NIL, an inhibitor of iNOS, was able to restore proliferation and neurogenesis in meningitis. L-NIL was given as an i.p. starting dose at the time of meningitis induction and was added to the drinking water for the remaining duration of the experiment. In animals receiving intrathecal PBS, the number of BrdU-positive cells at 3 days was not influenced by L-NIL treatment (Fig. 4A). Conversely, the reduction of proliferating cells associated with untreated meningitis was completely restored in meningitic animals receiving L-NIL. We performed double staining for BrdU and the early neuronal differentiation marker Hu-D to reveal changes of the rate of neuronally committed, newly formed cells (Fig. 4B). In these studies, L-NIL treatment of PBS-injected controls had no effect on the percentage of Hu-D and BrdU double-positive cells. While untreated meningitis was associated with a reduction of immature neurons, L-NIL treatment completely restored the percentage of Hu-D/BrdU-positive cells in meningitis mice. Additionally, we observed a strong reduction of the nitrotyrosine signal in L-NIL-treated meningitis mice (Fig. 3M). These data suggest that iNOS-derived NO mediates the reduction of proliferation and neurogenesis at 3 days after meningitis but is not involved in the regulation of baseline proliferation and neurogenesis.

Effect of iNOS inhibition in behavioral tests. We asked whether the restoration of proliferation and neuronal differentiation by L-NIL treatment of meningitis animals had a chronic functional correlate. In the Morris water maze paradigm, we were not able to detect a significant difference at 3 weeks after surgery between meningitis mice and PBS-injected controls regarding the decrease of escape latencies during the acquisition phase, swim speed, or motivation to escape. Remarkably, neither meningitis nor control mice exhibited a significant preference for the platform quadrant in the probe trial, i.e., after removal of the target platform (data not shown). Also, in the inhibitory avoidance task, only a subset of control mice displayed good learning (step-through latency of above 180 s). The percentage of good learners was moderately reduced at 3 weeks after experimental meningitis, and this was reversed by chronic treatment with L-NIL, but none of these effects reached statistical significance (Fig. 4C). In the hole board test, L-NIL treatment of experimental meningitis had no significant effect on the habituation to a new environment (data not shown). These findings suggest that neuropsychological correlates of the neuronal loss are subtle and are not reliably detected in the mentioned standard tests. Poor performance of the control mice is a limiting factor. There was a weak trend suggesting that a negative effect of intracranial inflammation on memory retention may be present and may be reversed by chronic L-NIL treatment.

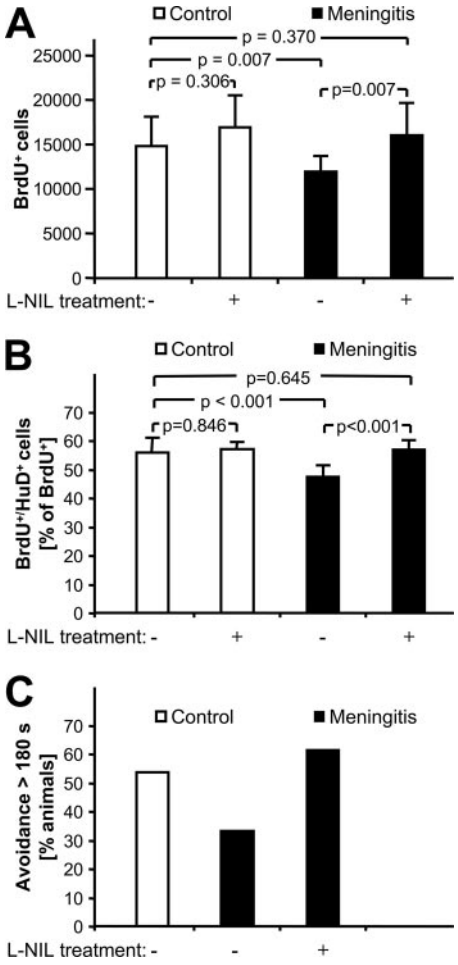

FIG. 4. Restoration of neurogenesis in the acute phase of meningitis by iNOS inhibition. (A) In nonmeningitic animals, the number of newly formed, BrdU-incorporating cells in the SGZ is not significantly changed by the specific iNOS inhibitor L-NIL. Control animals (open bars) and animals challenged with cell wall (solid bars) were treated with the iNOS inhibitor L-NIL as indicated. Neurogenesis was measured by BrdU-positive cells in both DG. (B) Early neuronal differentiation of BrdU-positive cells was demonstrated by Hu-D costaining. *P* values were calculated by Student-Newman-Keuls tests after one-way ANOVA. (C) Behavioral effect of L-NIL in the inhibitory avoidance paradigm 4 weeks after induction of experimental meningitis. Compared to PBS-treated controls, the proportion of animals avoiding the dark compartment of the test apparatus for more than 180 s (i.e., successful learners) has a tendency to be lower after challenge with PCW ($P = 0.26$), and this effect is abolished by chronic treatment with L-NIL ($P = 0.23$ versus untreated meningitis and $P = 1.0$ versus PBS-treated controls by Fisher's exact test).

DISCUSSION

Bacterial meningitis is a foremost infectious cause of neuronal degeneration of the hippocampus. Clinically, neuronal

damage is responsible for permanent neuropsychological disability in a large fraction of survivors. Here we report that not only are neurons killed during experimental meningitis but also adult neurogenesis is negatively affected by intracranial inflammation and cannot compensate for neuronal damage.

Induction of meningitis with highly purified PCW, a known Toll-like receptor 2 ligand, decreased neurogenesis during the acute phase of inflammation. Our results are supported by findings in a model of systemic inflammation, in which a reduction of immature neurons was reported 6 days after a single i.p. LPS injection (30). Given the systemic nature of the stimulus, it is not clear to what extent the reported effects on neurogenesis were related to the systemic or the intracranial inflammatory process in the latter study. Hence, an important aspect of our study is that we have demonstrated suppression of neurogenesis by strictly intracranial inflammation in a clinically relevant model of acute bacterial meningitis. Suppression of net neurogenesis was also reported in chronic brain inflammation induced by prolonged intracortical LPS infusion (12). In contrast to our results, those authors did not observe a reduction of BrdU-positive cells or BrdU/Doublecortin-positive neuroblasts, and they concluded that the net reduction of neurogenesis was due to an impaired survival of the newly formed neurons in the inflammatory setting.

Neurogenesis is a hypothetical source from which lost neurons might be replaced in bacterial meningitis, particularly since injury and neurogenetic capacity colocalize in the same brain region. Yet, for at least 5 weeks after meningitis we found a decreased total volume of the DG compared to that in controls. It is of note that we have used young adult mice in our experiments. While a significant increase of the neuronal cell count and DG volume was observed in the control animals, this increase was completely inhibited by PCW-induced meningitis. Clinically, this may point to an extended vulnerability of the developing CNS in bacterial meningitis.

Later in the course of recovery from intracranial inflammation, we observed a rebound increase of proliferation. More importantly, however, the increased proliferation was accompanied by a decrease in the percentage of newly formed cells adopting a neuronal phenotype. Thus, the net result of experimental meningitis is a net decrease of newly formed neurons early and at 3 weeks after induction of the inflammatory process through a combination of decreased proliferation and altered differentiation. Previous studies of neurogenesis in bacterial meningitis have reached conflicting results. In one study using live bacteria (18), a sharp increase of BrdU-positive nuclei in the DG was reported on day 2, followed by a gradual return to control levels on day 16, and more new neurons were generated on day 10. In a later study by the same group (46), no significant effect was reported at 30 h after infection, followed by a delayed increase in proliferation. An important difference from our study is the use of live bacteria, raising the possibility of a specific effect of bacterial metabolic products. Alternatively, quantification of BrdU-positive nuclei per DG area on selected sections rather than in the entire DG (as in our study) may be confounded by an uneven distribution of the baseline proliferation and of the inflammatory changes.

The reduction of BrdU-immunopositive cells on day 3 after induction of meningeal inflammation could be the result of several hypothetical events. Meningitis-associated neuronal loss, usually due to apoptosis, is particularly severe in the DG and often includes cells of the SGZ. Thus, loss of neuronal precursor cells (NPCs) could form a basis of reduced proliferation. Indeed, an increased vulnerability of precursor cells born 6 to 10 days before meningitis induction has recently been reported in a neonatal rat model of pneumococcal meningitis (20). In the present study, we did not detect colocalization of active caspase 3 with nestin or BrdU. Several factors may limit the validity of this finding. These include the weak expression of nestin in the perinuclear region (15) and the possibility that an unknown number of newly formed cells either could be cleared completely between S-phase labeling and sacrifice of the animals or could escape immunostaining in the presence of late apoptotic condensation. Still, our data do not provide support for loss of nestin-positive NPCs or of neurons born between challenge and sacrifice of the animal as a primary event in acute CNS inflammation, thus emphasizing inhibition of NPC proliferation as an alternative mechanism.

In regard to possible mediators of NPC inhibition by neuroinflammation, NO is a highly attractive candidate due to its role as a physiological negative regulator of NPC proliferation (8, 13, 34–38) and the well-established role of NO in the pathophysiology of bacterial meningitis. We were able to demonstrate iNOS immunoreactivity in microglia of the DG and hilus region 3 days after meningitis induction, with immunostaining for nitrotyrosine as a footprint for peroxynitrite, which is produced from NO under conditions of stress. Moreover, there was no overlap of areas of nitrotyrosine signal and BrdU incorporation. While bacterial surface components have been shown to induce release of NO from microglia in vitro (25), it is not known how meningitis leads to glial activation in the DG, as this brain region is probably not directly exposed to bacterial antigen. A hypothetical diffusion of proinflammatory molecules from the CSF space would be supported by three observations. First, neuronal damage in our experiments was usually concentrated in those parts of the DG situated nearest to the CSF space. Second, an acute suppression of proliferation was also observed in the SVZ, which is also located close to the ventricle. Third, the pneumococcal toxin pneumolysin was detected by immunostaining within the DG in a previous study, suggesting traffic of bacterial components in the intercellular space (6).

In experimental bacterial meningitis, NO has been identified as a mediator of blood flow increase, brain edema, and CSF pleocytosis (4, 5, 26, 44, 54). Regulation of iNOS in the brain tissue of meningitis animals was demonstrated on both the RNA (44) and protein (26) levels. The mechanisms involved in the antiproliferative effect of NO are not completely understood but appear to include formation of cGMP (2), upregulation of the cyclin-dependent kinase inhibitor p21 (38), and interaction with retinoblastoma and p53 systems (19). The restoration of neurogenesis by the specific iNOS inhibitor L-NIL suggests that local NO acts as a mediator reducing NPC proliferation in neuroinflammation. In support of the histological evidence, we observed a trend towards a functional improvement by L-NIL in the inhibitory avoidance paradigm. Memory impairment may reflect one of the neuropsychological deficits seen in patients after meningitis (3). A role of inflammatory glia in suppressing DG neurogenesis has been pointed out by two recent studies (12, 30), but inhibition of NPC pro-

liferation by NO as a major toxic glial product has not previously been demonstrated. The beneficial effects of minocycline and indomethacin treatment in these studies agree with a role of NO in NPC suppression. Minocycline acts as an inhibitor of microglial activation and has previously been shown to reduce iNOS expression, e.g., in global brain ischemia (58) or in a model of Huntington's disease (9). Indomethacin also reduced iNOS upregulation in cerebellar homogenates of LPS-treated rats (11). However, additional mediators may be involved in the modulation of neurogenesis in the context of inflammation. As an example, the tumor necrosis factor type 1 receptor has recently been reported to mediate reduced proliferation in the DG following status epilepticus (22).

In summary, precursor cell proliferation and adult neurogenesis are downmodulated in early PCW-induced meningitis. A delayed rebound increase of proliferation does not translate into a net gain of new neurons. Adult neurogenesis apparently cannot compensate for neuronal loss in the hippocampus. The cell wall-induced model of neuroinflammation is particularly well suited to dissect CNS processes affecting neuronal repair. Development of protective interventions to enhance neuronal repair will need to address how neuroinflammation inhibits both proliferation and neuronal differentiation, particularly through nitric oxide.

ACKNOWLEDGMENTS

This study was supported by the Deutsche Forschungsgemeinschaft (DFG), SFB 507, and the Meningitis Research Foundation as well as the Hermann and Lilly Schilling Foundation.

We do not have a commercial or other association that might pose a conflict of interest.

REFERENCES

1. **Bert, B., E. Dere, N. Wilhelmi, H. Kusserow, F. Theuring, J. P. Huston, and H. Fink.** 2005. Transient overexpression of the 5-HT_{1A} receptor impairs water-maze but not hole-board performance. Neurobiol. Learn. Mem. **84:** 57–68.
2. **Bogdan, C.** 2001. Nitric oxide and the regulation of gene expression. Trends Cell Biol. **11:**66–75.
3. **Bohr, V., O. B. Paulson, and N. Rasmussen.** 1984. Pneumococcal meningitis. Late neurologic sequelae and features of prognostic impact. Arch. Neurol. **41:**1045–1049.
4. **Boje, K. M.** 1995. Inhibition of nitric oxide synthase partially attenuates alterations in the blood-cerebrospinal fluid barrier during experimental meningitis in the rat. Eur. J. Pharmacol. **272:**297–300.
5. **Boje, K. M.** 1996. Inhibition of nitric oxide synthase attenuates blood-brain barrier disruption during experimental meningitis. Brain Res. **720:**75–83.
6. **Braun, J. S., J. E. Sublett, D. Freyer, T. J. Mitchell, J. L. Cleveland, E. I. Tuomanen, and J. R. Weber.** 2002. Pneumococcal pneumolysin and H_2O_2 mediate brain cell apoptosis during meningitis. J. Clin. Investig. **109:**19–27.
7. **Burns, K. A., and C. Y. Kuan.** 2005. Low doses of bromo- and iododeoxyuridine produce near-saturation labeling of adult proliferative populations in the dentate gyrus. Eur. J. Neurosci. **21:**803–807.
8. **Champlin, D. T., and J. W. Truman.** 2000. Ecdysteroid coordinates optic lobe neurogenesis via a nitric oxide signaling pathway. Development **127:** 3543–3551.
9. **Chen, M., V. O. Ona, M. Li, R. J. Ferrante, K. B. Fink, S. Zhu, J. Bian, L. Guo, L. A. Farrell, S. M. Hersch, W. Hobbs, J. P. Vonsattel, J. H. Cha, and R. M. Friedlander.** 2000. Minocycline inhibits caspase-1 and caspase-3 expression and delays mortality in a transgenic mouse model of Huntington disease. Nat. Med. **6:**797–801.
10. **Dash, P. K., S. A. Mach, and A. N. Moore.** 2001. Enhanced neurogenesis in the rodent hippocampus following traumatic brain injury. J. Neurosci. Res. **63:**313–319.
11. **Di Girolamo, G., M. Farina, M. L. Riberio, D. Ogando, J. Aisemberg, A. R. de los Santos, M. L. Marti, and A. M. Franchi.** 2003. Effects of cyclooxygenase inhibitor pretreatment on nitric oxide production, nNOS and iNOS expression in rat cerebellum. Br. J. Pharmacol. **139:**1164–1170.
12. **Ekdahl, C. T., J. H. Claasen, S. Bonde, Z. Kokaia, and O. Lindvall.** 2003. Inflammation is detrimental for neurogenesis in adult brain. Proc. Natl. Acad. Sci. USA **100:**13632–13637.
13. **Enikolopov, G., J. Banerji, and B. Kuzin.** 1999. Nitric oxide and Drosophila development. Cell Death Differ. **6:**956–963.
14. **Fallon, J., S. Reid, R. Kinyamu, I. Opole, R. Opole, J. Baratta, M. Korc, T. L. Endo, A. Duong, G. Nguyen, M. Karkehabadhi, D. Twardzik, S. Patel, and S. Loughlin.** 2000. In vivo induction of massive proliferation, directed migration, and differentiation of neural cells in the adult mammalian brain. Proc. Natl. Acad. Sci. USA **97:**14686–14691.
15. **Filippov, V., G. Kronenberg, T. Pivneva, K. Reuter, B. Steiner, L. P. Wang, M. Yamaguchi, H. Kettenmann, and G. Kempermann.** 2003. Subpopulation of nestin-expressing progenitor cells in the adult murine hippocampus shows electrophysiological and morphological characteristics of astrocytes. Mol. Cell Neurosci. **23:**373–382.
16. **Fischer, H., and A. Tomasz.** 1984. Production and release of peptidoglycan and wall teichoic acid polymers in pneumococci treated with beta-lactam antibiotics. J. Bacteriol. **157:**507–513.
17. **Garcia-Bustos, J. F., B. T. Chait, and A. Tomasz.** 1987. Structure of the peptide network of pneumococcal peptidoglycan. J. Biol. Chem. **262:**15400–15405.
18. **Gerber, J., T. Böttcher, J. Bering, S. Bunkowski, W. Bruck, U. Kuhnt, and R. Nau.** 2003. Increased neurogenesis after experimental Streptococcus pneumoniae meningitis. J. Neurosci. Res. **73:**441–446.
19. **Gibbs, S. M.** 2003. Regulation of neuronal proliferation and differentiation by nitric oxide. Mol. Neurobiol. **27:**107–120.
20. **Grandgirard, D., Y. D. Bifrare, S. J. Pleasure, J. Kummer, S. L. Leib, and M. G. Tauber.** 2007. Pneumococcal meningitis induces apoptosis in recently postmitotic immature neurons in the dentate gyrus of neonatal rats. Dev. Neurosci. **29:**134–142.
21. **Hoffmann, O., N. Keilwerth, M. B. Bille, U. Reuter, K. Angstwurm, R. R. Schumann, U. Dirnagl, and J. R. Weber.** 2002. Triptans reduce the inflammatory response in bacterial meningitis. J. Cereb. Blood Flow Metab. **22:** 988–996.
22. **Iosif, R. E., C. T. Ekdahl, H. Ahlenius, C. J. H. Pronk, S. Bonde, Z. Kokaia, S. E. W. Jacobsen, and O. Lindvall.** 2006. Tumor necrosis factor receptor 1 is a negative regulator of progenitor proliferation in adult hippocampal neurogenesis. J. Neurosci. **26:**9703–9712.
23. **Jin, K., M. Minami, J. Q. Lan, X. O. Mao, S. Batteur, R. P. Simon, and D. A. Greenberg.** 2001. Neurogenesis in dentate subgranular zone and rostral subventricular zone after focal cerebral ischemia in the rat. Proc. Natl. Acad. Sci. USA **98:**4710–4715.
24. **Kempermann, G., H. G. Kuhn, and F. H. Gage.** 1997. More hippocampal neurons in adult mice living in an enriched environment. Nature **386:**493–495.
25. **Lehnardt, S., L. Massillon, P. Follett, F. E. Jensen, R. Ratan, P. A. Rosenberg, J. J. Volpe, and T. Vartanian.** 2003. Activation of innate immunity in the CNS triggers neurodegeneration through a Toll-like receptor 4-dependent pathway. Proc. Natl. Acad. Sci. USA **100:**8514–8519.
26. **Leib, S. L., Y. S. Kim, S. M. Black, J. H. Tureen, and M. G. Tauber.** 1998. Inducible nitric oxide synthase and the effect of aminoguanidine in experimental neonatal meningitis. J. Infect. Dis. **177:**692–700.
27. **Li, N., S. Choudhuri, N. J. Cherrington, and C. D. Klaassen.** 2003. Down-regulation of mouse organic anion-transporting polypeptide 4 (Oatp4; Oatp1b2; Slc21a10) mRNA by lipopolysaccharide through the Toll-like receptor 4 (TLR4). Drug Metab. Dispos. **32:**1265–1271.
28. **Liu, J., K. Solway, R. O. Messing, and F. R. Sharp.** 1998. Increased neurogenesis in the dentate gyrus after transient global ischemia in gerbils. J. Neurosci. **18:**7768–7778.
29. **Mitchell, L., S. H. Smith, J. S. Braun, K. H. Herzog, J. R. Weber, and E. I. Tuomanen.** 2004. Dual phases of apoptosis in pneumococcal meningitis. J. Infect. Dis. **190:**2039–2046.
30. **Monje, M. L., H. Toda, and T. D. Palmer.** 2002. Inflammatory blockade restores adult hippocampal neurogenesis. Science **302:**1760–1765.
31. **Moore, W. M., R. K. Webber, G. M. Jerome, F. S. Tjoeng, T. P. Misko, and M. G. Currie.** 1994. L-*N*6-(1-Iminoethyl)lysine: a selective inhibitor of inducible nitric oxide synthase. J. Med. Chem. **37:**3886–3888.
32. **Nakatomi, H., T. Kuriu, S. Okabe, S. Yamamoto, O. Hatano, N. Kawahara, A. Tamura, T. Kirino, and M. Nakafuku.** 2002. Regeneration of hippocampal pyramidal neurons after ischemic brain injury by recruitment of endogenous neural progenitors. Cell **110:**429–441.
33. **Nau, R., A. Soto, and W. Brück.** 1999. Apoptosis of neurons in the dentate gyrus in humans suffering from bacterial meningitis. J. Neuropathol. Exp. Neurol. **58:**265–274.
34. **Packer, M. A., Y. Stasiv, A. Benraiss, E. Chmielnicki, A. Grinberg, H. Westphal, S. A. Goldman, and G. Enikolopov.** 2003. Nitric oxide negatively regulates mammalian adult neurogenesis. Proc. Natl. Acad. Sci. USA **100:** 9566–9571.
35. **Parent, J. M., T. W. Yu, R. T. Leibowitz, D. H. Geschwind, R. S. Sloviter, and D. H. Lowenstein.** 1997. Dentate granule cell neurogenesis is increased by seizures and contributes to aberrant network reorganization in the adult rat hippocampus. J. Neurosci. **17:**3727–3738.
36. **Peunova, N., and G. Enikolopov.** 1995. Nitric oxide triggers a switch to growth arrest during differentiation of neuronal cells. Nature **375:**68–73.
37. **Peunova, N., V. Scheinker, H. Cline, and G. Enikolopov.** 2001. Nitric oxide

is an essential negative regulator of cell proliferation in Xenopus brain. J. Neurosci. **21:**8809–8818.
38. **Poluha, W., C. M. Schonhoff, K. S. Harrington, M. B. Lachyankar, N. E. Crosbie, D. A. Bulseco, and A. H. Ross.** 1997. A novel, nerve growth factor-activated pathway involving nitric oxide, p53, and p21WAF1 regulates neuronal differentiation of PC12 cells. J. Biol. Chem. **272:**24002–24007.
39. **Reilly, C. M., L. W. Farrelly, D. Viti, S. T. Redmond, F. Hutchison, P. Ruiz, P. Manning, J. Connor, and G. S. Gilkeson.** 2002. Modulation of renal disease in MRL/lpr mice by pharmacologic inhibition of inducible nitric oxide synthase. Kidney Int. **61:**839–846.
40. Reference deleted.
41. **Scheld, W. M., R. G. Dacey, H. R. Winn, J. E. Welsh, J. A. Jane, and M. A. Sande.** 1980. Cerebrospinal fluid outflow resistance in rabbits with experimental meningitis. Alterations with penicillin and methylprednisolone. J. Clin. Investig. **66:**243–253.
42. **Schneider, O., U. Michel, G. Zysk, O. Dubuis, and R. Nau.** 1999. Clinical outcome in pneumococcal meningitis correlates with CSF lipoteichoic acid concentrations. Neurology **53:**1584–1587.
43. **Schröder, N. W., S. Morath, C. Alexander, L. Hamann, T. Hartung, U. Zähringer, U. B. Göbel, J. R. Weber, and R. R. Schumann.** 2003. Lipoteichoic acid (LTA) of Streptococcus pneumoniae and Staphylococcus aureus activates immune cells via Toll-like receptor (TLR)-2, lipopolysaccharide-binding protein (LBP), and CD14, whereas TLR-4 and MD-2 are not involved. J. Biol. Chem. **278:**15587–15594.
44. **Suzuki, Y., S. Fujii, T. Tominaga, T. Yoshimoto, S. Fujii, T. Akaike, H. Maeda, and T. Yoshimura.** 1999. Direct evidence of in vivo nitric oxide production and inducible nitric oxide synthase mRNA expression in the brain of living rat during experimental meningitis. J. Cereb. Blood Flow Metab. **19:**1175–1178.
45. **Tauber, M. G., H. Khayam-Bashi, and M. A. Sande.** 1985. Effects of ampicillin and corticosteroids on brain water content, cerebrospinal fluid pressure, and cerebrospinal fluid lactate levels in experimental pneumococcal meningitis. J. Infect. Dis. **151:**528–534.
46. **Tauber, S. C., C. Stadelmann, A. Spreer, W. Brück, R. Nau, and J. Gerber.** 2005. Increased expression of BDNF and proliferation of dentate granule cells after bacterial meningitis. J. Neuropathol. Exp. Neurol. **64:**806–815.
47. **Tomasz, A.** 1981. Surface components of Streptococcus pneumoniae. Rev. Infect. Dis. **3:**190–211.
48. **Tuomanen, E., H. Liu, B. Hengstler, O. Zak, and A. Tomasz.** 1985. The induction of meningeal inflammation by components of the pneumococcal cell wall. J. Infect. Dis. **151:**859–868.
49. **Tuomanen, E., A. Tomasz, B. Hengstler, and O. Zak.** 1985. The relative role of bacterial cell wall and capsule in the induction of inflammation in pneumococcal meningitis. J. Infect. Dis. **151:**535–540.
50. **van Praag, H., G. Kempermann, and F. H. Gage.** 1999. Running increases cell proliferation and neurogenesis in the adult mouse dentate gyrus. Nat. Neurosci. **2:**266–270.
51. **Vermeire, K., L. Thielemans, P. Matthys, and A. Billiau.** 2000. The effects of NO synthase inhibitors on murine collagen-induced arthritis do not support a role of NO in the protective effect of IFN-gamma. J. Leukoc. Biol. **68:**119–124.
52. **Voits, M., H. Fink, P. Gerhardt, and J. P. Huston.** 1995. Application of 'nose-poke habituation' validation with post-trial diazepam- and cholecystokinin-induced hypo- and hypermnesia. J. Neurosci. Methods **57:**101–105.
53. **Weber, J. R., D. Freyer, C. Alexander, N. W. Schröder, A. Reiss, C. Küster, D. Pfeil, E. I. Tuomanen, and R. R. Schumann.** 2003. Recognition of pneumococcal peptidoglycan, an expanded, pivotal role for LPS binding protein. Immunity **19:**269–279.
54. **Winkler, F., U. Koedel, S. Kastenbauer, and H. W. Pfister.** 2001. Differential expression of nitric oxide synthases in bacterial meningitis, role of the inducible isoform for blood-brain barrier breakdown. J. Infect. Dis. **183:**1749–1759.
55. **Yoshimura, A., E. Lien, R. R. Ingalls, E. Tuomanen, R. Dziarski, and D. Golenbock.** 1999. Cutting edge: recognition of Gram-positive bacterial cell wall components by the innate immune system occurs via Toll-like receptor 2. J. Immunol. **163:**1–5.
56. **Yoshimura, S., T. Teramoto, M. J. Whalen, M. C. Irizarry, Y. Takagi, J. Qiu, J. Harada, C. Waeber, X. O. Breakefield, and M. A. Moskowitz.** 2003. FGF-2 regulates neurogenesis and degeneration in the dentate gyrus after traumatic brain injury in mice. J. Clin. Investig. **112:**1202–1210.
57. **Yoshimura, S., Y. Takagi, J. Harada, T. Teramoto, S. S. Thomas, C. Waeber, J. C. Bakowska, X. O. Breakefield, and M. A. Moskowitz.** 2001. FGF-2 regulation of neurogenesis in adult hippocampus after brain injury. Proc. Natl. Acad. Sci. USA **98:**5874–5879.
58. **Yrjanheikki, J., R. Keinanen, M. Pellikka, T. Hokfelt, and J. Koistinaho.** 1998. Tetracyclines inhibit microglial activation and are neuroprotective in global brain ischemia. Proc. Natl. Acad. Sci. USA **95:**15769–15774.

Editor: J. N. Weiser